Shoji T, et al., J Genet Genomic Sci 2021, 6: 024
DOI: 10.24966/GGS-2485/100024

HSOA Journal of Genetics & Genomic Sciences

Research Article

Ribosome Profiling in *Streptococcus pneumoniae* Reveals the Role of Methylation of 23S rRNA Nucleotide G748 on Ribosome Stalling

Tatsuma Shoji[1]*, Akiko Takaya[2,3,4], Yoko Kusuya[5], Hiroki Takahashi[3,5,6] and Hiroto Kawashima[1]

[1]*Laboratory of Microbiology and Immunology, Graduate School of Pharmaceutical Sciences, Chiba University, Japan*

[2]*Department of Natural Products Chemistry, Graduate School of Pharmaceutical Sciences, Chiba University, Chiba, Japan*

[3]*Plant Molecular Science Center, Chiba University, Japan*

[4]*Medical Mycology Research Center, Chiba University, Japan*

[5]*Division of Bio-resources, Medical Mycology Research Center, Chiba University, Japan*

[6]*Molecular Chirality Research Center, Chiba University, Japan*

Abstract

Background: Many nucleotides in 23S rRNA are methylated post-transcriptional by methyltransferases and cluster around the Peptidyl Transferase Center (PTC) and the Nascent Peptidyl Exit Tunnel (NPET) located in 50S subunit of 70S ribosome. Biochemical interactions between a nascent peptide and the tunnel may stall ribosome movement and affect expression levels of the protein. However, no studies have shown a role for NPET on ribosome stalling using an NPET mutant.

Results: A ribosome profiling assay in *Streptococcus pneumoniae* demonstrates for the first time that an NPET mutant exhibits completely different ribosome occupancy compared to wild-type. We demonstrate, using RNA foot printing that changes in ribosome occupancy correlate with changes in ribosome stalling. Further, statistical analysis shows that short peptide sequences that cause ribosome stalling are species-specific and evolutionarily selected. PET structure is required to realize these specie-specific ribosome stalling.

Conclusion: Results support the role of NPET on ribosome stalling. NPET structure is required to realize the species-specific and evolutionary conserved ribosome stalling. These findings clarify the role of NPET structure on the translation process.

Keywords: Ribosome stalling; Ribosome profiling; Ribosomopathy; 23S rRNA modification; *Streptococcus pneumoniae*

***Corresponding author:** Tatsuma Shoji, Laboratory of Microbiology and Immunology, Graduate School of Pharmaceutical Sciences, Chiba University, Japan, Tel: +81 8051809605; E-mail: tatsumashoji@bioinforest.com

Citation: Shoji T, Takaya A, Kusuya Y, Takahashi H, Kawashima H (2021) Ribosome Profiling in *Streptococcus pneumoniae* Reveals the Role of Methylation of 23S rRNA Nucleotide G748 on Ribosome Stalling. J Genet Genomic Sci 6: 024.

Received: February 15, 2021; **Accepted:** February 18, 2021; **Published:** February 25, 2021

Background

Endogenous rRNA modifying enzymes methylate or pseudouridylate specific rRNA nucleotides at functionally important regions in the ribosome, such as the Peptidyl Transferase Center (PTC) [1]. Approximately one-third of modified residues of 23S rRNA are clustered around the Nascent Peptide Exit Tunnel (NPET) [2].While the role of rRNA modification remains unclear, though it is generally believed that they have fine-tune functions of the ribosome in translation [3], especially under the stress conditions [4], via the biochemical interactions between the nascent peptide and tunnel [5,6]. These interactions may stall ribosome movement and thus affect the expression level of the protein [6]. However, no studies have shown the role of NPET in ribosome stalling using an NPET mutant.

Some modifications of NPET are important for determining antibiotic resistance or susceptibility [7,8]. While the role of the methylation at G748 (m^1G748) in *Streptococcus pneumoniae* remains unclear, we previously showed that inactivation of the methyltransferase $RlmA^{II}$, which methylates the N-1 position of nucleotide G748 located near the PTC, results in increased resistance to telithromycin (TEL) in erm (B)-carrying *S .pneumoniae* [7].

We explored the role of NPET structure in translation initially by establishing the ribosome profiling assay in *S. pneumonia* and investigating ribosomal distribution in both wild-type and $RlmA^{II}$-deficient *S. pneumoniae*. Subsequent analysis showed that m^1G748 is responsible for ribosome stalling and plays a role in species specificity.

Results

The loss of N-1 methylation at G748 greatly changes the distribution of ribosome's

We constructed two *S. pneumonia* mutant strains, Sp284 and Sp379 to investigate the role of NPET. Sp284 is a $RlmA^{II}$-disrupted mutant harboring pTKY1111 encoding tlr *B* of the S1 strain [7]. Sp379 is an $RlmA^{II}$-disrupted mutant harboring pTKY1127 encoding tlrB of Sp44 [7]. The latter strains display no methyltransferase activity because of

the C23R mutation [7]. The difference between Sp284 and Sp379 is only the capability to methylate G748.

We also performed a deep sequencing-based ribosome profiling analysis in Sp284 and Sp379. Ribosome profiling captures a global snapshot of ribosome positioning and density on template mRNAs with single-nucleotide resolution. The erm (B) operon, where ribosomes stall at the ermBL region [9], was selected, for example, to examine the distribution of ribosomes (Figure 1A). Ribosome position and density in the erm(B) operon in Sp379 was completely different from positions and density in Sp284 (Figure 1A).

The difference in the ribosome occupancy between two strains in erm (B) operon led us to speculate a general role of m^1G748 in the translation process. Ribosome density across all ORFs in Sp379 was higher than in Sp284, especially around the latter region, indicating an important role of m^1G748 in the translation process, with differences in ribosome position and density across all Open Reading Frames (ORFs) being assessed using a metagene analysis (Figure 1B).

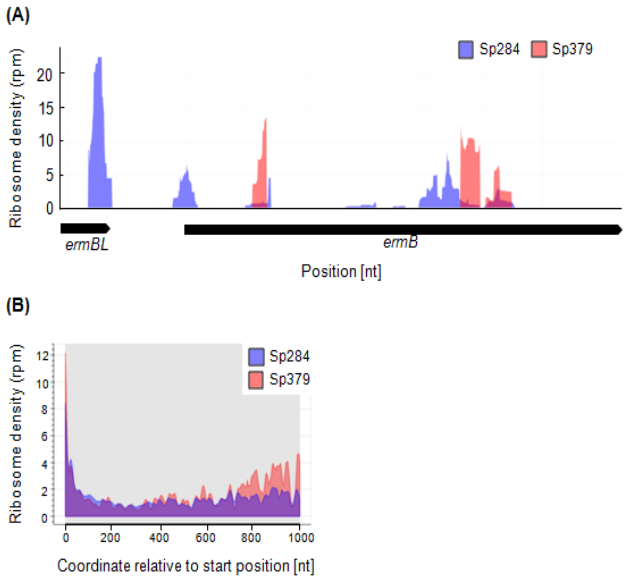

Figure 1: Differences in ribosome density (RD) profiles between Sp284 and Sp379.

(A) RD in erm(B) in Sp284 or Sp379. (B) Metagene profile of RD in Sp284 or Sp379. RD across all ORFs was aligned relative to the start position.

m^1G748 affects ribosome stalling

A high number of Ribosome-Protected Footprints (RPFs) mappings to the transcriptome (mRNA-seq) at a unique position are indicative of ribosome stalling [10]. Thus, observed global changes implya role for m^1G748 in ribosome stalling.

We tested this hypothesis by first constructing erm(B) operon-over expression *s. pneumoniae* strains Sp380 and Sp382 from Sp284 and Sp379 respectively, to clarify differences between Sp284 and Sp379 (Tables 1 and 2).We then probed ribosomes of Sp380 and Sp382 before and after extracting total RNA with dimethyl sulfate.

Strain	Relevant characteristics	Reference of source
Streptococcus pneumoniae		
S1	TEL resistance clinical isolate	[7]
Sp36	TEL-resistant mutants of S1 isolated from 8 μg/mL TEL-containing BHI-Y agar plates	[7]
Sp274	ΔtlrB::aad(9) in S1	[7]
Sp284	Sp274 harboring pTKY1111	This study
Sp379	Sp274 harboring pTKY1127	This study
Sp380	S1 harboring pTKY1041	This study
Sp382	Sp274 harboring pTKY1041	This study

Table 1: Bacterial strains.

Plasmid	Relevant characteristics	Reference of source
pUC18	Cloning vector	Lab. collection
pLZ12-Km^2	Shuttle vector	[11]
pTKY862	pLZ12-Km2 with Sp resistant cassette ad(9)	[12]
pTKY1041	pLZ12-Km2 with 1401 bperm(B) fragment from S1	[7]
pTKY1109	pUC18 with 328 bptlrB fragment	[7]
pTKY1110	pUC18 with disrupted tlrB fragment by insertion of an Sp resistant cassette aad(9)	[7]
pTKY1111	pLZ12-Km2 with 1065 bptlrB fragment from S1	[7]
pTKY1127	pLZ12-Km2 with 1065 bptlrB fragment from Sp44	[7]

Table 2: Plasmids.

Figure 2A shows the secondary mRNA structure from the ermBL region that was previously demonstrated [9]. Consistent with this report, nucleotides in the stems were protected from chemical modification when probing after extracting total RNA in both Sp380 and Sp382 strains. Conversely, these regions were not protected when probing before extracting total RNA in Sp380 (Figure 2B), but these regions remained unprotected in Sp382 (Figure 2B). Stems were likely disrupted in Sp380 *in vivo* presumably due to ribosome stalling in the ermBL region. m^1G748 affects such stalling.

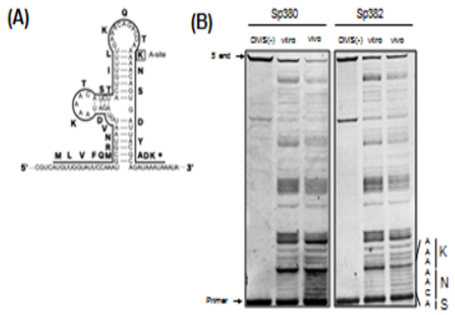

Figure 2: RNA foot printing assay for the ermBL region.

(A) The secondary structure model of ermBL region in erm(B) mRNA suggested in [9]. Amino acids in at the A-site of stalled ribosomes in the ermBL region are boxed. (B) RNA foot printing of the ermBL region indicates a difference in ribosome stalling between Sp380 and Sp382. DMS was added to bacterial cultures (in vivo) or the total RNAs (in vitro). Reactions were quenched, and total RNA was purified and used in primer extension assays to detect base modifications. Unmodified RNA was used as a control (DMS (-)). The gel shows primer extension products from bases 117 to 152. The sequence around the calculated P-site and encoded amino acids are indicated on the side of the gel.

Characterization of effects of m^{1}G748 on ribosome stalling

Ribosome stalling does not always mean an end to translation. Translation resumes in some cases [13,14]. Such cases are termed "transient stalling" [15] and may contribute to co translational protein and be evolutionarily preferred [16,17]. In contrast, "strong stalling" does not appear to restart and requires rescue [18,19]. We examined the type of ribosome stalling affected by m^{1}G748 byfirst defining A-site peaks (see Methods for details) and counted the number of A-site peaks across all CDSs (Figures 3A and 3B). Two populations observed in Sp284 (Figure 3A) were consistent with a previous report [18]. However, surprisingly, almost no transient stalling was observed in Sp379 (Figure 3B), indicating a role for m^{1}G748 for keeping transient stalling. A slight decrease in the number of peaks of strong stalling was observed compared to Sp284 (Figures 3A and 3B).

Stalling peptides were identified as previously described [15] to further examine the role of m^{1}G748 on strong stalling. Briefly, we defined strong stalling as described in Methods and collected nascent peptide sequences in the exit tunnel for strong stalling events. We then calculated the probability of occurrence for 8,000 tripeptides and defined stalling peptides as tripeptides with a probability higher than 0.9999. Surprisingly, few stalling peptides were common between Sp284 and Sp379 (Figure 3C), suggesting that the position of "strong stalling" is different between the two strains.

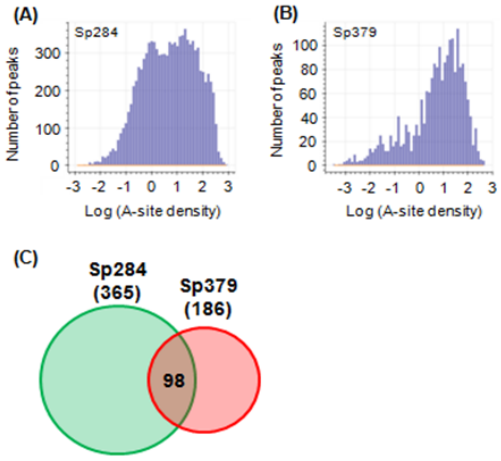

Figure 3: The effect of m1G748 on transient stalling and strong stalling.

(A,B) Histograms showing the distribution of A-site density in Sp284 and Sp379, respectively. (C) Venn diagram for stalling peptide sequences in Sp284 and Sp379. The number of stalling peptide sequences is shown in parentheses. The number in the intersection region reflects common stalling peptides.

Several known stalling peptides, such as PPP, KKK and KKR, are common among some organisms, including *Saccharomyces cerevisiae* and *Escherichia coli* [20,21]. However, stalling peptides in Sp284 and Sp379 did not include these previously reported molecules [see Additional file 1], indicating that ribosome stalling is species-specific.

m^{1}G748 is required to realize evolutionarily conserved ribosome stalling

Stalling peptides in *S. pneumonia* were different in previous reports, which led us to speculate on how they are distributed in the proteome. We examined relationships between stalling peptides and proteome in *S. pneumoniae*, by initially identifying 360 of over-represented and 382 under-represented examples for three amino acids in the *S. pneumoniae* proteome as previously [15]. Enrichment of over-and under-represented tripeptides in stalling peptides was investigated using Fisher's exact test (Figure 4). Over-represented peptides were significantly enriched in the set from Sp379, with under-represented peptides being significantly enriched in the stalling peptide set of Sp284, indicating that the strong stalling is not evolutionarily favored [see Additional file 2].m1G748 is likely required to realize evolutionarily conserved ribosome stalling.

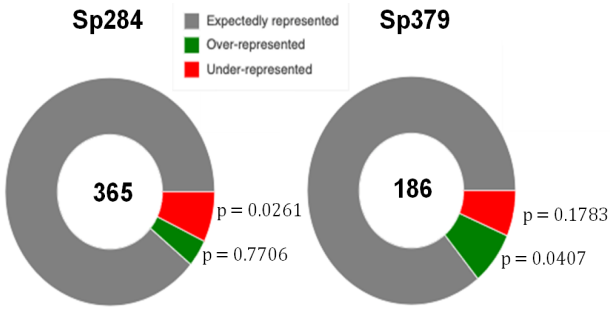

Figure 4: Enrichment of over- and under-represented stalling peptides.

The number of the stalling peptides is represented at the center of the donut. The p-value represents statistical significance of the over- and under-represented fractions.

Discussion

We investigated the role of NPET in translation using a ribosome profiling assay in *S. pneumoniae*. The finding that the loss of the methyl group at m^{1}G748 had a notable impact on the distribution of the ribosomes and ribosome stalling (Figures 1 and 2) highlights the importance of the NPET structure and explains why rRNA modifications are clustered near the PTC and NPET. The role of NPET using other NPET mutants will be investigated in the future.

Alteration of NPET results in changes to the stalling peptide set (Figure 3C). Thus, translation depends not only on mRNA sequence but also on the structure of NPET. Prediction of ribosome stalling based only on mRNA sequence would be difficult. Using NPET information is crucial because the structure of the NPET is not necessarily unique in a cell [22], with some studies having tried to predict ribosome occupancy or stalling [21,23], and performance of developed software could be improved with additional parameters for NPET structure.

A global change in stalling position may result in a global effect on cell proteome. This effect might explain why RlmA^{II} mutants of *S. pnuemoniae* are rarely clinically isolated [24]. The loss of the m^{1}G748 methyl group inhibits binding of telithromycin to the exit tunnel [7] and may also cause a decrease in fitness of *S. pneumonia* in a clinical setting. This concept might be useful since antibiotics that compromise targets that maintain healthy ribosomes would not cause resistant bacteria.TEL-resistant *S. pneumoniae* ribosomes are unhealthy.

The ribosomopathy encompasses diseases caused by abnormalities in the structure or function of ribosomal proteins or rRNA genes or

other genes whose products are involved in ribosome biogenesis [25-27]. Skeletal muscle atrophy [28], Diamond–Blackfan anemia [26] and Treacher Collins syndrome [26] are examples of ribosomopathy. However, no reports regarding exit tunnel-induced ribosomopathy exist. The present study examined *S. pneumoniae*; however, exit tunnel-derived ribosomopathy might be common among organisms, including humans. For example, ribosomal protein L17 (RPL17) is up regulated in parallel with stress vulnerability [29]. RPL17 is located near the end of the exit tunnel [22]. Therefore, RPL17 could be responsible for ribosome stalling. This concept, exit-tunnel-induced ribosomopathy, might explain the mechanism of the disorder in the future.

Conclusion

We demonstrate the role of m^1G748 on ribosome stalling in *S. pneumoniae*. m^1G748 is required to realize species-specific and evolutionarily conserved stalling. The loss of the methyl group at m^1G748 has a great impact on the distribution of the ribosomes and ribosome stalling, and results in exit-tunnel-induced ribosomopathy. This might be the reason why $RlmA^{II}$ mutants of *S. pnuemoniae* are rarely clinically isolated. This study is the first to show the role of NPET using an NPET mutant. These findings clarify the role of NPET structure on the translation process.

Methods

Bacterial strains, plasmids, and media

Bacterial strains and plasmids are shown in tables 1 and 2, respectively. *S. pneumoniae* strain S1 with reduced TEL susceptibility (MIC, 2μg/ml) was clinically isolated in Japan [7]. Pneumococci were routinely cultured at 37°Cand 5% CO_2 in air in a brain-heart infusion with 0.5% yeast extract (BHI-Y) broth and BHI-Y agar, supplemented with 5% horse blood. *E. coli* was grown in L broth (1% bact-tryptone, 0.5% bact yeast extract, 0.5% sodium chloride, pH 7.4) and L agar. When necessary, medium was supplemented with kanamycin (25–500μg/mL), spectinomycin (100 μg/mL) and ampicillin (25 μg/mL).

Transformation

Synthetic Competence-Stimulating Peptide (CSP) 1 and the method of Iannelli and Pozzi [30] were used to transform *S. pneumoniae* S1 into a transformation-competent state.

RNA-Seq

S. pneumoniae cultures were grown to log-phase; 2.8 mL of cultures were added to 2.8 mL of 100°C preheated RNA lysis buffer (1% SDS, 0.1 M NaCl and 8mM EDTA) and vortexed for 2min. The resulting lysates were added to 5.6 mL of 100°C preheated acid phenol (Sigma-Aldrich) and vortexed for 5 min. After centrifuging, RNA was extracted from the aqueous phase using DirectZol (Zymo Research). rRNA was removed from total RNA using MICROB Express (Ambion). Resulting total mRNA (400ng as an input) was used for constructing the DNA library, using KAPA Stranded RNA-Seq Library Preparation Kit Illumina platforms (KK8400). DNA libraries were sequenced using the Illumina HiSeq 1500 system and single-end reads. Illumina libraries were preprocessed by clipping the Illumina adapter sequence using Trimmomatic v.0.39 [31] and then aligned to the S1 genome sequence [7] using HISAT2 v.2.2.1 [32].

Ribo-Seq

Libraries were prepared as previously described with some modifications (see below) [10].

Cell growth and harvest: *S. pneumoniae* cultures (2.4L) were grown to log-phase. Cells were pretreated for 2 min with 100 μg/mL chloramphenicol. Immediately after chloramphenicol pretreatment, cultures were placed on ice. Cells were pelleted by centrifugation at 8,000 ×g for 15 min at 4°C. After decanting the supernatant, cell pellets were resuspended in 2.5 mL of prechilled resuspension buffer [10mM $MgCl_2$, 100mM NH_4Cl, 20mM Tris (pH 8.0), and 1mM chloramphenicol].

Lysate preparation and Nuclease digestion: Cells were sonicated on ice and centrifuged at 12,000 × g for 10 min at 4°C. Aliquots of lysate, containing 25 Abs_{260} ribosome units (1 A_{260} = 12 μg/μL) [5] were digested with 60 U of MNase (Roche) and 60 U of SUPERase. In (Ambion) with the addition of chloramphenicol to a final concentration of 1mM to remove unprotected mRNA and generate footprint fragments. Digestion reactions were incubated for 1 h at 25°C and quenched with the addition of EGTA to a final concentration of 6 mM.

Sucrose fractionation: Linear sucrose gradients [5-40% (wt/vol)] were prepared with 7.6mL of buffer A and buffer B [10mM $MgCl_2$, 100mM NH_4Cl, 2mM DTT, 20mM, 0.2 mMchloramphenicol, Tris pH 7.8 and 5% or 40% Sucrose, respectively], by loading Buffer B on Buffer A in 16PA tube and placed vertically for 12 hr at 4°C the placed horizontally for 2 hr at 4°C.

Digested samples were carefully loaded onto prepared gradients and centrifuged at 124,700 × g for 8 hr at 4°C in a P28S2 rotor. Sucrose gradients were fractionated manually into 200 μL portions and $A_{260}$was recorded for each fraction. Absorbance values were graphed in Microsoft Excel to determine ribosome footprint associated fractions (RPF fractions). RPF were consequently pooled.

Ribosome footprint preparation: RNA was purified from RPF using the SDS/hot acid phenol. Three mL of samples were first denatured with SDS to a final concentration of 1% (wt/vol) and 2.7mL of preheated acid phenol (65°C) (Sigma-Aldrich). Mixtures were vortexed for 5 min at 65°C. After centrifuging, aqueous phases were mixed with one volume of acid phenol, and 0.9 volumes of chloroform/isoamyl alcohol (24:1). RNA was precipitated with ethanol and resuspended in 10 μL of 10mM Tris (pH 8.0).

Ribosome footprint samples were resolved on denaturing polyacrylamide gels for size selection of footprint fragments. RNA samples were prepared for electrophoresis by adding 2x Novex TBE-Urea Sample Buffer (Invitrogen). Ladder standards used a 0.05 μg/μL 10-bp DNA Ladder (Invitrogen), prepared in 2x Novex TBE-Urea Sample Buffer and 10mM Tris (pH 8.0). Samples were resolved on a 15% TBE-Urea gel in 1 × TBE buffer for 65 min at 200V. Gels were stained for 3 min with SYBR Gold Nucleic Acid Gel Stain (diluted from 10,000x in 1x TE; Invitrogen) and visualized by UV transillumination. A band between 20 and 45 was excised using the 10-bp DNA ladder to identify footprint fragments. RNA was recovered using the ZR small-RNA PAGE Recovery Kit (Zymo Research) following the manufacturer's protocol, except that RNA was eluted from the final spin column with 15 μL of 10mM Tris (pH 8.0). Collected RNA was quantified and characterized by using a small-RNA chip on the Agilent BioAnalyzer (Agilent Technologies).

Dephosphorylation: Three hundred pmol of footprints were denatured for 2min at 80°C and placed on ice. The 3' ends were dephosphorylated with T4 polynucleotide kinase (T4 PNK; NEB) in the following reaction mix: 1 × T4 PNK reaction buffer (without ATP), 20 U SUPERase. In and 10 U T4 PNK. Reactions were incubated at 37°C for 1 hr. The enzyme was then heat-inactivated for 10 min at 75°C. RNA was precipitated with isopropanol and resuspended in 10 µL of 10mM Tris (pH 8.0).

Linker-1 Ligation: Twenty pmolof dephosphorylated RNA was prepared by diluting with 10mM Tris (pH 8.0). One µg of Linker-1 (5'-App CTGTAGGCACCATCAAT ddC-d') was added to RNA samples. Mixtures were denatured for 90 s at 80°C, then cooled to room temperature for 15 min. Ligation of RNA to Linker-1 used the following reaction components: 20% (wt/col) PEG, 10% DMSO, 1 × T4 Ligase reaction buffer, 20U SUPERase. In, and 10 U T4 Ligase 2, truncated (NEB). Reaction mixtures were incubated at 37°C for 1 h. 2 × TBE-Urea sample buffer was added to reaction mixtures. Samples were resolved on a 10% TBE-Urea gel in 1 × TBE buffer at 200V. Gels were stained for 3min in SYBR Gold Nucleic Acid Gel Stain and visualized by UV transillumination. A band between 30 and 70 nt was excised using the 10-bp DNA ladder to mark ligated product size. Ligated RNA was recovered using the ZR small-RNA PAGE Recovery kit. Ligated products were eluted from the final spin column with 6 µL of 10mM Tris (pH 8.0).

Phosphorylation: The collected 3' ligated samples were incubated for 2 min at 80°C and placed on ice. The 5' ends were phosphorylated by T4 PNK in the following reaction mix: 1 × T4 PNK Reaction Buffer, 20 U SUPERase. In 10 U T4 PNK and 1mM ATP. Reactions were incubated at 37°C for 1 hr. The enzyme was heat-inactivated for 10 min at 75°C. RNA was precipitated with isopropanol and resuspended in 6 µL of 10mM Tris (pH 8.0).

Linker-2 ligation: 1 µL of 100 µM Linker-2(5'-GAGTCTGCGTG TGATTCGGGTTAGGTGTTGGGTTGGGCCA-3') was added to phosphorylate RNA samples. Mixtures were denatured for 15 min at 65°C and placed on ice. Ligation of RNA to Linker-2 used the following reaction mix: 17.5% (wt/vol) PEG, 1 × T4 ligase reaction buffer, 20U SUPERase. In, and 10 U T4 RNA Ligase1 (NEB). Reaction mixtures were incubated at 37°C for 2.5 h. Two × TBE-Urea sample buffer was added and ligated RNA resolved on 10% TBE-Urea gels in 1 × TBE buffer at 200V. Gels were stained for 3min in SYBR Gold Nucleic Acid Gel Stain and visualized by UV transillumination. A band between 90 and 120 nt was excised using the 10-bp DNA ladder to identify ligated products. Ligated RNA was recovered using the ZR small-RNA PAGE Recovery kit. Products were eluted from the final spin column with 6 µL of 10mM Tris (pH 8.0).

Reverse transcription: Four point five µL of ligated samples were mixed with 1 µL of 0.1 µM Linker-1-RT (5'-ATTGATGGTGCCTACAG-3') and 1 µL of 0.5mM dNTP. The resulting mixtures were denatured for 2 min at 80°C then quickly cooled on ice. Samples were incubated at room temperature for 10 min reverse transcription using Superscript III Reverse Transcriptase (Invitrogen) with the following reaction mix: 1 × first strand buffer, 5mMDTT, 20 U SUPERase. In and 200 U Superscript III Reverse Transcriptase. Reaction mixtures (10 µL) were incubated for 1hr at 47°C. RNA products were hydrolyzed by adding 1mMNaOH to a final concentration of 0.1 mM and incubated for 15 min at 95°C. cDNA products were resolved from the unextended primer on a 10% TBE-Urea gel in 1 × TBE buffer at 200V. Samples were prepared for electrophoresis by adding 2 × TBE-Urea sample buffers and denaturing for 5 min at 95°C. Gels were stained for 3 min in SYBR Gold Nucleic Acid Gel Stain and visualized by UV transillumination. A band between 90 and 120 nt was excised using the 10-bp DNA ladder to identify reverse transcription products. DNA was recovered using the ZR small-RNA PAGE Recovery Kit. cDNA products were eluted from the final spin column with 6 µL of 10mM Tris (pH 8.0).

2nd strand DNA synthesis: cDNA (100 pg) was amplified with Q5 High Fidelity Polymerase (NEB) using LInker-2-partial (5'-TTAGGTGTTGGGTTGGGCCA-3') and Linker-1 as primers. Amplified PCR products were purified using AMPure Bead (Beackman Coulter). Double-stranded DNA was eluted from beads with 10 µL of 10mM Tris (pH 8.0).

Library preparation and sequencing: KAPA Hyper Prep Kits from Illumina (KK8500) were used to construct the library with a slight modification to the manufacturer's protocol. The manufacturer's protocol followed the EndRepair and A-tailing steps, where, briefly, 5 µL of KAPA frag buffer was added to 45 µL of purified double-stranded DNA. The resulting DNA library was quantified and characterized using the high-sensitivity DNA chip on an Agilent BioAnalyzer (Agilent Technologies). Libraries were sequenced using an Illumina HiSeq 1500 system and single-end reads after adding PhiX (Illumina) to a final concentration of 30% (vol/vol) to improve sequencing quality.

Sequence analysis: Illumina libraries were preprocessed by clipping adapter sequence (Linker-1 and Linker-2) using TrimmomaticPE v.0.39 [31] for the Illumina adapters and CutAdapt v.2.10 [33] for linker sequences. Sequencing reads were aligned to the S1 genome sequence [7] using HISAT2 v.2.2.1 [32]. The S1 gene feature file [7] was used to identify the CDS region. Sequencing data were deposited in the DDBJ database with accession number DRA011224.

Definition of the ribosome density

The Ribosome Density (RD) was calculated as previously described [34], except that ribosome footprints between 24 and 30 nt were selected for calculations. This range was chosen to assess as many footprints as possible to improve statistical power and to exclude fragments suspected not to represent footprints (see Additional file 3 for the detail).

Metagene analysis

Each normalized RD profile was aligned by its start cod on and averaged across each position, with RD profiles first being scaled by their own mean density to obtain metagene profiles (Figure 1B).

DMS modification of ribosomes

Dimethyl Sulfate (DMS) modification was based on a previously published protocol [7]. *S. pneumoniae* cultures (2.4L) were grown to log-phase. Cells were pelleted by centrifugation at 8,000 × g for 15 min at 4°C and washed and resuspended in 250 µL of DMS buffer [10mM $MgCl_2$, 50mM sodium cacodylate pH 7.0]. For the modification *in vivo*, DMS solution was added to a final concentration of 50mM and incubated for 1hr at 20°C. The reaction was quenched by the addition of 62.5 µL ice-cold stop buffer [1M β-mercaptoethanol

and 1.5M sodium acetate, pH 7.0]. RNA was extracted using SDS/hot acid phenol method. Preheated (100°C) acid phenol (0.9 volumes) was added to the quenched mixture and vortexed for 5 min. After centrifugation, RNA was purified from the aqueous phase using DirectZol (Zymo Research). For the modification *in vitro*, RNA was first extracted from the cell suspension using the same method as for *in vivo*. After purifying the total RNA, DMS solution was added to a final concentration of 50mM in DMS buffer and incubated for 1hr at 20°C then quenched. RNA was precipitated with ethanol and resuspended in 20 µL of 10 mM Tris (pH 8.0).

Primer extension

The degree of methylation of each RNA was assayed by primer extension initially described by Morgan et al., [35]. Briefly, 210 µg of DMS-probed total RNA, 400 nM concentration of an oligonucleotide primer containing 5' - linked fluoresce in isothiocyanate (FITC) (5'-[FITC]GAATTAATCTAACGTATTTATTTATCTGCGTAATCA -3'), and 500 µM dNTP were mixed, heated to 95°C for 1 min, and cooled to allow annealing at 53°C. A mixture containing Superscript III Reverse Transcriptase was added, and the reaction was continued at 53°C for an additional 20 min. Reactions were terminated by the addition of 2 × TBE-Urea sample buffer after incubation at 70°C for 15 min. Extension products were resolved on a 12.5% TBE-urea gel and visualized using a TyphoonFLA9000 photoimager (GE Healthcare).

Definition of A-site peaks

We first determined the A-site corresponding to each read by an offset of [(15/27)×(L)] from the 5' end of the read, where L is the length of each read. Then we used normalized A-site count (ribo/mRNA) as A-site peaks.

Definition of strong stalling

Strong stalling is defined as A-site peaks with a height of higher than eight because the number of A-site peaks in the ermBL region was around eight. This region is where ribosome stalling was confirmed by RNA foot printing. The results, however, remain robust also for other cutoff values of A-site density.

Enrichment of over-, under-represented peptide sequence

Over- and under-represented peptide sequences were identified as previously described [13], except that *p*-value cutoff is 0.0001 for under-represented peptides and 0.9999 for over-represented peptides.

Supplementary Information

Additional file 1: Supplementary Tables S1
Additional file 2: Supplementary Tables S2
Additional file 3: Supplementary Figure S1

Declarations

Ethics approval and consent to participate

Not applicable.

Consent for publication

Not applicable.

Availability of data and materials

All data generated in this study have been deposited to the DDBJ depository (DRA011224).

Competing interests

The authors declare that they have no competing interests.

Funding

This work was funded by Grant-in-Aid for Japan Society for the Promotion of Science Research Fellow 16J02984

Author contributions

ST contributed to the conception and overall design of the work, all of experiments, bioinformatics analysis and interpretation of Ribo-Seq data and drafting of the manuscript. TA contributed to the design of Ribo-Seq experiments. KY contributed to Ribo-Seq experiments. TH contributed to bioinformatics analysis, interpretation of Ribo-Seq data, drafting of the manuscript and substantial revision of the manuscript. YT contributed to the drafting of the manuscript. KH contributed to the conception and overall design of the work, interpretation of data, and drafting and revision the manuscript. The authors read and approved the final manuscript.

Acknowledgment

We thank Tomoko Yamamoto for discussions and comments to the manuscript.

References

1. Xiong L, Shah S, Mauvais P, Mankin AS (1999) A ketolide resistance mutation in domain II of 23S rRNA reveals the proximity of hairpin 35 to the peptidyl transferase centre. Mol Microbiol 31: 633-639.
2. Kannan K, Mankin AS (2011) Macrolide antibiotics in the ribosome exit tunnel: species-specific binding and action. Ann N Y Acad Sci 1241: 33-47.
3. Sloan KE, Warda AS, Sharma S, Entian K-D, Lafontaine DLJ, et al. (2011) Modifications of ribosomal RNA: From enzymes to function. RNA Biol 14: 97-110.
4. Baldridge KC, Contreras LM (2014) Functional implications of ribosomal RNA methylation in response to environmental stress. Crit Rev Biochem Mol Biol 49: 69-89.
5. Nakatogawa H, Ito K (2002) The ribosomal exit tunnel functions as a discriminating gate. Cell 108: 629-636.
6. Tenson T, Ehrenberg M (2002) Regulatory nascent peptides in the ribosomal tunnel. Cell 108: 591-594.
7. Takaya A, Sato Y, Shoji T, Yamamoto T (2013) Methylation of 23S rRNA nucleotide G748 by RlmAII methyltransferase renders Streptococcus pneumoniae telithromycin susceptible. Antimicrob Agents Chemother 57: 3789-3796.
8. Shoji T, Takaya A, Sato Y, Kimura S, Suzuki T, et al. (2015) RlmCD-mediated U747 methylation promotes efficient G748 methylation by methyltransferase RlmAII in 23S rRNA in Streptococcus pneumoniae; interplay between two rRNA methylations responsible for telithromycin susceptibility. Nucleic acids research 43: 8964-8972.
9. Min Y-H, Kwon A-R, Yoon E-J, Shim MJ, Choi EC (2008) Translational attenuation and mRNA stabilization as mechanisms of erm (B) induction by erythromycin. Antimicrobial agents and chemotherapy 52: 1782-1789.

10. Davis AR, Gohara DW, Yap MNF (2014) Sequence selectivity of macrolide-induced translational attenuation. Proc Natl Acad Sci USA 111: 15379-15384.

11. Okada N, Tatsuno I, Hanski E, Caparon M, Sasakawa C (1998) Streptococcus pyogenes protein F promotes invasion of HeLa cells. Microbiology 144: 3079-3086.

12. Takaya A, Kitagawa N, Kuroe Y, Endo K, Okazaki M, et al. (2010) Mutational analysis of reduced telithromycin susceptibility of Streptococcus pneumoniae isolated clinically in Japan. FEMS microbiology letters 307: 87-93.

13. Kimchi-Sarfaty C, Oh JM, Kim IW, Sauna ZE, Calcagno AM, et al. (2007) "A" silent" polymorphism in the MDR1 gene changes substrate specificity. Science 315: 525-528.

14. Tsai C-J, Sauna ZE, Kimchi-Sarfaty C, Ambudkar SV, Gottesman MM, et al. (2008) Synonymous mutations and ribosome stalling can lead to altered folding pathways and distinct minima. J Mol Biol 383: 281-291.

15. Sabi R, Tuller T (2017) Computational analysis of nascent peptides that induce ribosome stalling and their proteomic distribution in Saccharomyces cerevisiae. Rna 23: 983-994.

16. Ciryam P, Morimoto RI, Vendruscolo M, Dobson CM, O'Brien EP (2013) In vivo translation rates can substantially delay the cotranslational folding of the Escherichia coli cytosolic proteome. Proc Natl Acad Sci USA 110.: 132-140.

17. Döring K, Ahmed N, Riemer T, Suresh HG, Vainshtein Y, et al. (2017) Profiling Ssb-nascent chain interactions reveals principles of Hsp70-assisted folding. Cell 170: 298-311.

18. Richter JD, Coller J (2015) Pausing on polyribosomes: make way for elongation in translational control. Cell 163: 292-300.

19. Moore SD, Sauer RT (2005) Ribosome rescue: tmRNA tagging activity and capacity in Escherichia coli. Mol Microbiol 58: 456-466.

20. Charneski CA, Hurst LD (2013) Positively charged residues are the major determinants of ribosomal velocity. PLoSBiol 11: 1001508.

21. Liu TY, Song YS (2016) Prediction of ribosome footprint profile shapes from transcript sequences. Bioinformatics 32: 183-191.

22. Wang M, Parshin AV, Shcherbik N, Pestov DG (2015) Reduced expression of the mouse ribosomal protein Rpl17 alters the diversity of mature ribosomes by enhancing production of shortened 5.8 S rRNA. RNA 21: 1240-1248.

23. Zhang S, Hu H, Zhou J, He X, Jiang T (2017) Analysis of ribosome stalling and translation elongation dynamics by deep learning. Cell systems 5: 212-220.

24. Kataja J, Seppälä H, Huovinen P (2001) In vitro activities of the novel ketolide telithromycin (hmr 3647) against erythromycin-resistant streptococcusspecies. Antimicrob Agents Chemother 45: 789-793.

25. Nakhoul H, Ke J, Zhou X, Liao W, Zeng SX, et al. (2014) Ribosomopathies: mechanisms of disease. Clin Med Insights Blood Disord 7: 7-16.

26. Narla A, Ebert BL (2010) Ribosomopathies: human disorders of ribosome dysfunction. Blood 115: 3196-3205.

27. Keersmaecker KD, Sulima SO, Dinman JD (2015) Ribosomopathies and the paradox of cellular hypo-to hyperproliferation. Blood 125: 1377-1382.

28. Connolly M, Paul R, Farre-Garros R, Natanek SA, Bloch S, et al. (2018) miR-424-5p reduces ribosomal RNA and protein synthesis in muscle wasting. J Cachexia Sarcopenia Muscle 9: 400-416.

29. Hori H, Nakamura S, Yoshida F, Teraishi T, Sasayama D, et al. (2018) Integrated profiling of phenotype and blood transcriptome for stress vulnerability and depression. J Psychiatr Res 104: 202-210.

30. Iannelli F, Pozzi G (2004) Method for introducing specific and unmarked mutations into the chromosome of Streptococcus pneumoniae. Molecular biotechnology 26: 81-86.

31. Bolger A, Giorgi F (2014) Trimmomatic: a flexible read trimming tool for illumina NGS data. Bioinformatics 30: 2114-2120.

32. Kim D, Paggi JM, Park C, Bennett C, Salzberg SL (2019) Graph-based genome alignment and genotyping with HISAT2 and HISAT-genotype. Nature biotechnology 37: 907-915.

33. Martin M (2011) Cutadapt removes adapter sequences from high-throughput sequencing reads. EMBnet journal 17: 10-12.

34. Basu A, Yap MNF (2016) Ribosome hibernation factor promotes Staphylococcal survival and differentially represses translation. Nucleic acids research 44: 4881-4893.

35. Sigmund CD, Ettayebi M, Borden A, Morgan EA (1988) Antibiotic resistance mutations in ribosomal RNA genes of Escherichia coli. Methods in enzymology. Academic Press 164: 673-690.

Supplementary Files

Stalling peptides in Sp284	Stalling peptides in Sp379	Common Stalling peptides
AAA	AAR	EYN
AAC	AAV	KVQ
AAD	ADQ	PKP
AAE	AEE	ERG
AAI	AEK	EKP
AAK	AFN	KKV
AAL	AKA	NGR
AAP	AKK	GDF
AAR	APA	KAA
AAT	APK	QQP
AAV	APP	NSA
ADN	APQ	NWG
ADQ	ARQ	DFA
AEE	ARR	TGK
AEI	ATD	KKA
AEK	ATH	LGR
AEQ	ATR	VAV
AFR	AVA	TPA
AGA	CCN	EYC
AGP	CNR	WGD
AHA	CNW	AEE
AHI	DFA	EPE
AHV	DGP	AAV
AIK	DHG	RRV
AKA	DHN	APK
AKG	DIP	YTG
AKK	DQM	TAA
AKP	DQQ	TDG
AKR	DTG	ERK
AKV	EAD	PHT
ANE	EAV	KPA
ANP	EEY	RVG
APA	EHK	TQQ
APE	EKP	WYV
APG	EKS	VDH
APK	EKT	IRH
APQ	EPE	PVR
APV	ERG	GAA
AQW	ERK	HKK
ARG	EYC	HEG
ARQ	EYN	RRS
ARR	FAK	PKA
AST	FTG	KRH
ATD	FTK	ARQ
ATE	FVN	AVA
ATG	GAA	ADQ
ATH	GCN	IPS
ATR	GDF	DQQ
ATT	GGC	GCN
AVA	GHI	DHG
AVE	GKR	RRL
AVG	GKV	SLT
AVK	GPH	EAV
AVN	GQV	KRA
AVS	GRR	PEK
AYT	GSY	QQA
CNW	GTG	PAP
CTT	HEG	RGG
DAA	HGH	GGC
DFA	HGK	KAE
DGP	HIL	RRA
DHG	HKE	KVW
DNE	HKK	AEK
DPH	HRR	QPP
DQQ	HSF	MKR
DRW	HVD	RHR
DTA	IEP	CNW
DTG	IGH	AAR
DVE	IKT	PTP
DWM	INV	MAK
DYA	IPS	AKK
EAD	IRH	HVD
EAN	KAA	INV
EAP	KAE	DGP
EAV	KCC	SAN
EET	KDV	RKH
EGA	KKA	PAE
EGD	KKV	APQ
EGG	KNK	RGK
EGP	KPA	GTG
EGV	KPK	GSY
EHR	KRA	PPK
EIN	KRG	ATR
EKA	KRH	TGS
EKP	KRV	RGL
ENN	KTE	QQQ
EPE	KVQ	APA
EQF	KVW	ARR
EQH	KWY	DTG
EQP	LDG	NEP
ERG	LGR	SAQ
ERK	MAK	EAD
ETH	MKR	YAR
ETP	MRV	ATD
ETR	MVE	AKA
EVA	NAV	ATH
EVN	NDA	HRR
EYC	NEP	RVT
EYN	NGR	
FRA	NHG	
FRR	NRH	
GAA	NSA	

GAK	NVK	
GCN	NVV	
GDF	NWG	
GEG	PAE	
GGA	PAP	
GGC	PEK	
GGG	PGQ	
GGR	PHR	
GGS	PHT	
GHA	PKA	
GIK	PKK	
GIT	PKP	
GKA	PPK	
GPK	PPV	
GPT	PSY	
GRK	PTP	
GRY	PVR	
GSA	QPP	
GSV	QPS	
GSY	QQA	
GTE	QQP	
GTG	QQQ	
GTW	REK	
GVA	RGG	
GVK	RGK	
GYN	RGL	
HAA	RHR	
HAD	RKH	
HEG	RNT	
HID	RQA	
HIW	RQF	
HKK	RRA	
HQR	RRL	
HRR	RRQ	
HRT	RRS	
HTD	RRV	
HVD	RSE	
HVE	RVD	
HVP	RVG	
HWI	RVR	
IAA	RVT	
IIA	RYT	
INV	SAN	
IPS	SAQ	
IRH	SKN	
ITI	SLT	
IVE	SPQ	
KAA	SYR	
KAE	TAA	
KAG	TDG	
KAH	TEG	
KAV	TEH	
KAY	TGK	
KEV	TGS	

KGG	TKN	
KGS	TPA	
KGT	TPG	
KKA	TPT	
KKG	TQQ	
KKP	TRR	
KKV	TSK	
KPA	TWE	
KPG	VAG	
KRA	VAV	
KRF	VCY	
KRH	VDH	
KSA	VDI	
KSK	VEP	
KTK	VKP	
KTV	VNH	
KVQ	VNI	
KVW	VTP	
KYE	VWI	
LAR	WAT	
LGR	WEI	
LKA	WGD	
LRR	WIK	
LTA	WYV	
MAH	YAR	
MAK	YCT	
MAN	YNR	
MDN	YRG	
MDW	YRV	
MKR	YTG	
MLA		
MNT		
MQP		
MRG		
MRT		
NAA		
NAE		
NAK		
NEM		
NEP		
NES		
NGA		
NGR		
NKP		
NNH		
NQP		
NSA		
NTK		
NTT		
NVN		
NVP		
NWG		
PAE		
PAL		

PAN		
PAP		
PEA		
PEK		
PEP		
PGG		
PGH		
PGS		
PHE		
PHT		
PHV		
PKA		
PKP		
PKV		
PMA		
PPH		
PPK		
PQP		
PSW		
PTP		
PTR		
PTS		
PVA		
PVR		
PWR		
QAE		
QMD		
QNE		
QPE		
QPK		
QPP		
QPT		
QQA		
QQP		
QQQ		
QRA		
QRV		
QSG		
QVA		
QWR		
RAK		
RAR		
RAS		
RDS		
REF		
RFR		
RGG		
RGI		
RGK		
RGL		
RHG		
RHR		
RHT		
RHY		

RIN		
RKH		
RPH		
RPR		
RPT		
RQG		
RQK		
RRA		
RRE		
RRL		
RRN		
RRP		
RRS		
RRV		
RSP		
RTA		
RTG		
RVE		
RVG		
RVT		
RWN		
SAA		
SAN		
SAQ		
SAV		
SCT		
SHR		
SLT		
STK		
SVA		
SVM		
TAA		
TAH		
TAQ		
TDG		
TDT		
TDV		
TEA		
TGA		
TGK		
TGP		
TGR		
TGS		
TGT		
TGW		
THK		
TKA		
TKE		
TKT		
TPA		
TPH		
TPR		
TQQ		
TRL		

TSH		
TST		
TTT		
TVV		
TWQ		
TYK		
VAA		
VAE		
VAS		
VAV		
VDH		
VEA		
VEG		
VEK		
VES		
VEY		
VGE		
VGG		
VGR		
VGT		
VIP		
VIS		
VKA		
VKK		
VKT		
VKV		
VMD		
VNV		
VVF		
WGD		
WIT		
WKQ		
WME		
WRG		
WRQ		
WYV		
WYY		
YAH		
YAR		
YCK		
YED		
YEH		
YET		
YNA		
YQP		
YTG		
YVV		

Table S1: The list of stalling peptides.

The first and the second columns list stalling peptides in Sp284 and Sp379 respectively. The third column shows the list of stalling peptides that are common between strains.

Over-represented prptides	Under-represented peptides
ACG	AAE
ACS	AAP
ADF	AAT
ADK	ADP
ADY	ADT
AEK	AEP
AGF	AES
AGI	AGP
AGL	AKF
AGV	ANE
AIL	APP
AKE	ASE
AKN	AVP
ALA	CCC
AQA	CCD
ASH	CCW
ASQ	CHC
ATG	CHW
AYQ	CKC
CFE	CMQ
CHP	CMR
CHY	CMW
CSK	CPM
DEV	CQC
DFD	CVW
DFE	CWP
DFF	CYW
DFI	DAN
DFL	DAQ
DFP	DDE
DFS	DDG
DFV	DDN
DFY	DDP
DGK	DDR
DGQ	DDT
DGT	DEG
DIP	DGG
DKI	DGP
DKV	DHD
DLA	DHK
DLD	DIG
DLP	DND
DNL	DNE
DNP	DNK
DQV	DPG
DRI	DPP
DYF	DRE
DYH	DRG
DYI	DSA
DYL	DSE
DYQ	DTE
DYY	DTG
EAG	DTK

EAI	DTQ
EDF	DVG
EDL	DVS
EEA	EDD
EEI	EDE
EEL	EDN
EEV	EDP
EIA	EDQ
EIL	EDR
EKE	EDS
EKG	EDT
EKI	EEP
EKL	EFK
EKM	EGE
EKR	EGG
EKT	EGP
EKV	EGS
EKY	EHE
ELA	EPA
ENG	EPD
ENI	EPE
ENL	EPG
ENP	EPK
ENQ	EPN
EQA	EPP
EQI	EPQ
EQV	EPR
ERF	EQH
ERI	EQN
ERL	EQQ
ETG	EQR
EVV	ESA
FAK	ESE
FCQ	ESK
FDE	ESN
FDK	EST
FDN	ETQ
FDQ	EWD
FEE	EYE
FEN	EYK
FER	EYN
FKN	EYT
FNP	FEY
FNQ	FII
FSD	FIM
FSP	FKF
FVT	FKI
FWN	FKL
FYQ	FKV
GAG	FKY
GCG	FLI
GCS	FMF
GFD	FML
GFS	FMS

GIP	FMY
GIS	FQL
GKI	FRL
GKS	FRV
GKT	FYV
GLP	GAA
GLT	GAE
GNP	GAQ
GQT	GCW
GQV	GDA
GRI	GDD
GSG	GDP
GTG	GEA
GTP	GEG
GVD	GEQ
HCF	GGD
HFS	GKA
HFT	GLQ
HHF	GNE
HHL	GNK
HPD	GPA
HPE	GPD
HYH	GPE
HYP	GPF
HYQ	GPI
IAG	GPK
IAQ	GPL
IAR	GPP
IAS	GPQ
IEE	GTN
IEK	GTQ
IEN	GWC
IFP	HCM
IIG	HCW
IKE	HDD
ILA	HED
ILP	HND
ILS	HNE
INQ	HNN
IPA	HWW
IPE	IEF
IPN	IEI
IPT	IEP
IPV	IEY
IQE	III
IRD	IIK
IRK	IIL
IRQ	IIY
ISQ	IKF
ISR	IKI
ISS	IKL
IYQ	IKM
KDF	IKV
KDG	IKY

KDL	ILI
KDY	ILY
KEA	IMF
KEE	IMI
KEI	IML
KEK	IMY
KEL	INI
KEN	IQI
KEV	ITL
KHC	IVV
KIA	IWC
KKE	IYI
KKI	KCE
KKV	KCK
KKW	KDD
KNG	KFE
KNP	KFF
KNR	KFK
KQV	KFL
KRI	KFM
KRL	KFP
KRV	KFQ
KTI	KFR
KTV	KFS
KWY	KFT
LAD	KGA
LAE	KGP
LAG	KGS
LAK	KHE
LAQ	KHK
LAS	KHT
LDE	KLM
LDK	KLQ
LDY	KME
LEE	KPP
LEK	KQQ
LEN	KSA
LGI	KSE
LKD	KYT
LKE	KYV
LKK	LEF
LKN	LEL
LLA	LEP
LNP	LEY
LNQ	LFI
LPE	LFK
LPF	LFM
LPS	LGE
LPV	LGP
LPY	LHV
LRE	LHW
LSD	LII
LSG	LIK
LSK	LIL

LSN	LIM
LSQ	LKC
LSR	LKF
LTD	LKI
LTE	LKL
LTP	LKM
LYQ	LKV
MKE	LKY
MKI	LLI
MKK	LLL
MKQ	LLM
MKR	LLW
MLE	LLY
MNQ	LMF
MRQ	LML
MSK	LMY
MSR	LNF
MTK	LQF
MTS	LQI
NGI	LQL
NGK	LQM
NGQ	LQQ
NGR	LQW
NHQ	LRI
NIP	LRL
NLP	LRM
NLS	LRT
NLT	LRV
NPA	LVI
NPD	LWV
NPE	LYI
NPF	LYM
NPK	LYV
NPN	MCH
NPQ	MCW
NPS	MEP
NPT	MFI
NPY	MHV
NQE	MLI
NQF	MLL
NQL	MLY
NQV	MYC
NRF	MYE
NRL	MYF
NRV	MYI
NRY	MYK
NYL	MYV
PDF	NAT
PEE	NDD
PEK	NDS
PEN	NDT
PIL	NED
PKT	NEF
PNC	NEG

PSQ	NEH
PVF	NEK
PVI	NES
PVL	NGP
PVY	NIN
QAG	NKF
QAI	NND
QAL	NNE
QAY	NSA
QDL	NSM
QEI	NST
QEK	PCY
QEL	PFR
QGI	PGE
QKI	PGL
QTI	PKF
QTV	PLK
QVA	PLQ
QVL	PLR
RDY	PPA
RFG	PPD
RQA	PPE
RYF	PPG
RYQ	PPK
SGG	PPP
SGK	PPQ
SKE	PPV
SKH	PQR
SLA	PYE
SLS	QCC
SPE	QGP
SQA	QKS
SQE	QND
SQT	QPG
SSS	QQD
SWY	QQN
SYL	QQS
TDE	QSE
TGK	QSN
TGW	QWC
THF	QYK
TIA	RAD
TIL	RAP
TPD	RCC
TPE	REP
TPV	RGD
TSP	RGP
TVE	SAA
TVL	SAG
TWY	SAN
VAT	SDA
VDG	SED
VEK	SEL
VEN	SEP

VKD	SES
VKE	SGP
VLA	SNE
VLD	SPG
VLP	SPP
VLS	STE
VNP	TEG
VPV	TEY
VSS	TGP
VTS	TKF
VVD	TKG
WEN	TKL
WKE	TKM
WQE	TKS
WYQ	TLQ
WYY	TMY
YCH	TQL
YDF	TRS
YFD	TTQ
YHF	VEY
YHP	VII
YLD	VIL
YPD	VKF
YQA	VKI
YQD	VKL
YQE	VKM
YQG	VLI
YQH	VLL
YQK	VQL
YQL	VVL
YQN	VYK
YQT	WAA
YQV	WCC
YRE	WCE
YRK	WCH
YYL	WCT
YYQ	WHC
	WPC
	WPG
	WPH
	WPW
	WQC
	WWC
	WWM
	WWP
	WWW
	YCC
	YEF
	YEL
	YEY
	YIV
	YKI
	YKL
	YKS

	YKY
	YML
	YVI
	YVM
	YWC

Table S2: The list of over- and under-represented peptides.

The first and the second columns list over-represented peptides and under-represented peptides in *S. pneumoniae* proteome composition.

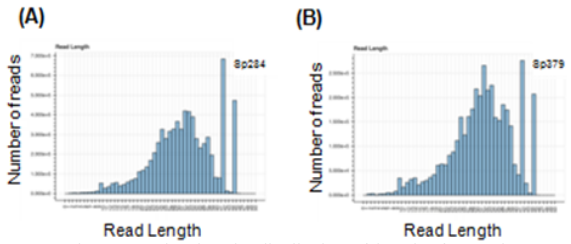

Figure S1: Histograms showing the distribution of length of RFPs in Sp284 and Sp379, respectively.

HERALD

Advances In Industrial Biotechnology | ISSN: 2639-5665

Advances In Microbiology Research | ISSN: 2689-694X

Archives Of Surgery And Surgical Education | ISSN: 2689-3126

Archives Of Urology

Archives Of Zoological Studies | ISSN: 2640-7779

Current Trends Medical And Biological Engineering

International Journal Of Case Reports And Therapeutic Studies | ISSN: 2689-310X

Journal Of Addiction & Addictive Disorders | ISSN: 2578-7276

Journal Of Agronomy & Agricultural Science | ISSN: 2689-8292

Journal Of AIDS Clinical Research & STDs | ISSN: 2572-7370

Journal Of Alcoholism Drug Abuse & Substance Dependence | ISSN: 2572-9594

Journal Of Allergy Disorders & Therapy | ISSN: 2470-749X

Journal Of Alternative Complementary & Integrative Medicine | ISSN: 2470-7562

Journal Of Alzheimers & Neurodegenerative Diseases | ISSN: 2572-9608

Journal Of Anesthesia & Clinical Care | ISSN: 2378-8879

Journal Of Angiology & Vascular Surgery | ISSN: 2572-7397

Journal Of Animal Research & Veterinary Science | ISSN: 2639-3751

Journal Of Aquaculture & Fisheries | ISSN: 2576-5523

Journal Of Atmospheric & Earth Sciences | ISSN: 2689-8780

Journal Of Biotech Research & Biochemistry

Journal Of Brain & Neuroscience Research

Journal Of Cancer Biology & Treatment | ISSN: 2470-7546

Journal Of Cardiology Study & Research | ISSN: 2640-768X

Journal Of Cell Biology & Cell Metabolism | ISSN: 2381-1943

Journal Of Clinical Dermatology & Therapy | ISSN: 2378-8771

Journal Of Clinical Immunology & Immunotherapy | ISSN: 2378-8844

Journal Of Clinical Studies & Medical Case Reports | ISSN: 2378-8801

Journal Of Community Medicine & Public Health Care | ISSN: 2381-1978

Journal Of Cytology & Tissue Biology | ISSN: 2378-9107

Journal Of Dairy Research & Technology | ISSN: 2688-9315

Journal Of Dentistry Oral Health & Cosmesis | ISSN: 2473-6783

Journal Of Diabetes & Metabolic Disorders | ISSN: 2381-201X

Journal Of Emergency Medicine Trauma & Surgical Care | ISSN: 2378-8798

Journal Of Environmental Science Current Research | ISSN: 2643-5020

Journal Of Food Science & Nutrition | ISSN: 2470-1076

Journal Of Forensic Legal & Investigative Sciences | ISSN: 2473-733X

Journal Of Gastroenterology & Hepatology Research | ISSN: 2574-2566

Journal Of Genetics & Genomic Sciences | ISSN: 2574-2485

Journal Of Gerontology & Geriatric Medicine | ISSN: 2381-8662

Journal Of Hematology Blood Transfusion & Disorders | ISSN: 2572-2999

Journal Of Hospice & Palliative Medical Care

Journal Of Human Endocrinology | ISSN: 2572-9640

Journal Of Infectious & Non Infectious Diseases | ISSN: 2381-8654

Journal Of Internal Medicine & Primary Healthcare | ISSN: 2574-2493

Journal Of Light & Laser Current Trends

Journal Of Medicine Study & Research | ISSN: 2639-5657

Journal Of Modern Chemical Sciences

Journal Of Nanotechnology Nanomedicine & Nanobiotechnology | ISSN: 2381-2044

Journal Of Neonatology & Clinical Pediatrics | ISSN: 2378-878X

Journal Of Nephrology & Renal Therapy | ISSN: 2473-7313

Journal Of Non Invasive Vascular Investigation | ISSN: 2572-7400

Journal Of Nuclear Medicine Radiology & Radiation Therapy | ISSN: 2572-7419

Journal Of Obesity & Weight Loss | ISSN: 2473-7372

Journal Of Ophthalmology & Clinical Research | ISSN: 2378-8887

Journal Of Orthopedic Research & Physiotherapy | ISSN: 2381-2052

Journal Of Otolaryngology Head & Neck Surgery | ISSN: 2573-010X

Journal Of Pathology Clinical & Medical Research

Journal Of Pharmacology Pharmaceutics & Pharmacovigilance | ISSN: 2639-5649

Journal Of Physical Medicine Rehabilitation & Disabilities | ISSN: 2381-8670

Journal Of Plant Science Current Research | ISSN: 2639-3743

Journal Of Practical & Professional Nursing | ISSN: 2639-5681

Journal Of Protein Research & Bioinformatics

Journal Of Psychiatry Depression & Anxiety | ISSN: 2573-0150

Journal Of Pulmonary Medicine & Respiratory Research | ISSN: 2573-0177

Journal Of Reproductive Medicine Gynaecology & Obstetrics | ISSN: 2574-2574

Journal Of Stem Cells Research Development & Therapy | ISSN: 2381-2060

Journal Of Surgery Current Trends & Innovations | ISSN: 2578-7284

Journal Of Toxicology Current Research | ISSN: 2639-3735

Journal Of Translational Science And Research

Journal Of Vaccines Research & Vaccination | ISSN: 2573-0193

Journal Of Virology & Antivirals

Sports Medicine And Injury Care Journal | ISSN: 2689-8829

Trends In Anatomy & Physiology | ISSN: 2640-7752